JACS
JOURNAL OF THE AMERICAN CHEMICAL SOCIETY

Article

pubs.acs.org/JACS

Bio-orthogonal Coupling as a Means of Quantifying the Ligand Density on Hydrophilic Quantum Dots

Naiqian Zhan,[†] Goutam Palui,[†] Jan-Philip Merkl,[†,‡] and Hedi Mattoussi*[,†]

[†]Department of Chemistry and Biochemistry, Florida State University, 95 Chieftan Way, Tallahassee, Florida 32306, United States
[‡]Institute of Physical Chemistry, University of Hamburg, Grindelallee 117, 20146 Hamburg, Germany

Supporting Information

ABSTRACT: We describe the synthesis of two metal-coordinating ligands that present one or two lipoic acid (LA) anchors, a hydrophilic polyethylene glycol (PEG) segment and a terminal reactive group made of an azide or an aldehyde, two functionalities with great utility in bio-orthogonal coupling techniques. These ligands were introduced onto the QD surfaces using a combination of photochemical ligation and mixed cap exchange strategy, where control over the fraction of azide and aldehyde groups per nanocrystal can be easily achieved: LA-PEG-CHO, LA-PEG-N_3, and bis(LA)-PEG-CHO. We then demonstrate the application of two novel bio-orthogonal coupling strategies directly on luminescent quantum dot (QD) surfaces that use click chemistry and hydrazone ligation under catalyst-free conditions. We applied the highly efficient hydrazone ligation to couple 2-hydrozinopyridine (2-HP) to aldehyde-functionalized QDs, which produces a stable hydrazone chromophore with a well-defined optical signature. This unique optical feature has enabled us to extract a measure for the ligand density on the QDs for a few distinct sizes and for different ligand architectures, namely mono-LA-PEG and bis(LA)-PEG. We found that the foot-print-area per ligand was unaffected by the nanocrystal size but strongly depended on the ligand coordination number. Additionally, we showed that when the two bio-orthogonal functionalities (aldehyde and azide) are combined on the same QD platform, the nanocrystal can be specifically reacted with two distinct targets and with great specificity. This design yields QD platforms with distinct chemoselectivities that are greatly promising for use as carriers for in vivo imaging and delivery.

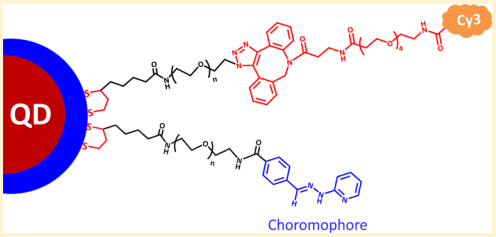

INTRODUCTION

Integration of luminescent semiconductor nanocrystals (quantum dots, QDs) into biology for use as tagging agents and/or sensing platforms is greatly promising.[1−6] It exploits some of the unique physical and optical properties that these materials exhibit, such as tunable emission and great photochemical stability.[7] However, this requires postgrowth modification to render the QDs hydrophilic and biocompatible, as these materials are often prepared using high temperature growth route and are thus hydrophobic. Several strategies have been developed to modify the QD surfaces and promote their dispersion in aqueous media.[8−12] One strategy exploits the ability of certain coordinating groups to interact with the metal-rich surface of the nanocrystals and employs ligand exchange, where the native cap is substituted with bifunctional coordinating ligands to promote hydrophilicity.[10,13−16] These bifunctional ligands typically present one or more anchoring groups that coordinate onto the QD surfaces and a hydrophilic moiety to promote affinity to buffer media. The ligand exchange strategy is easy to implement and allows control over the coordination interactions between the nanocrystals and ligands, as well as the number of reactive groups per QD; it also provides QDs with compact hydrodynamic size. Dihydrolipoic acid (DHLA) and its derivatives have been used in designing ligands with high affinity to ZnS-overcoated QDs.[10,14,17] For instance, our group has developed several molecular scale ligands presenting one or two lipoic acid anchors appended with either a polyethylene glycol (PEG) short chain or a zwitterion group (LA-PEG, LA-ZW, bis(LA)-PEG, and bis(LA)-ZW) and applied them for stabilizing both luminescent QDs and Au nanoparticles.[10,14,18,19] This route has yielded dispersions of QDs and AuNPs with good colloidal stability over a wide range of conditions.[14,18,19] Additionally, the PEG moiety can be modified with specific terminal functionalities to facilitate the bioconjugation of the nanoparticles with target molecules such as dyes, peptides, proteins, and redox complexes.[14,15,20−22]

Several conventional conjugation techniques have been developed to couple biomolecules to various inorganic nanocrystals, including EDC condensation reaction (amine to carboxylic acid), thiol−ene reaction, and avidin−biotin binding.[8,23,24] These approaches, though ubiquitous, have some limitations. For example, EDC coupling uses excess amounts of precursors and coupling reagents, which require careful removal of the byproducts and excess reagents; it may also cause cross-linking.[25] As alternative to these routes, there has been a growing interest in developing bio-orthogonal coupling chemistries directly on the nanocrystal surfaces, because these routes are rapid, selective, and can be carried out under mild

Received: December 30, 2015
Published: February 8, 2016

© 2016 American Chemical Society

DOI: 10.1021/jacs.5b13574
J. Am. Chem. Soc. 2016, 138, 3190−3201

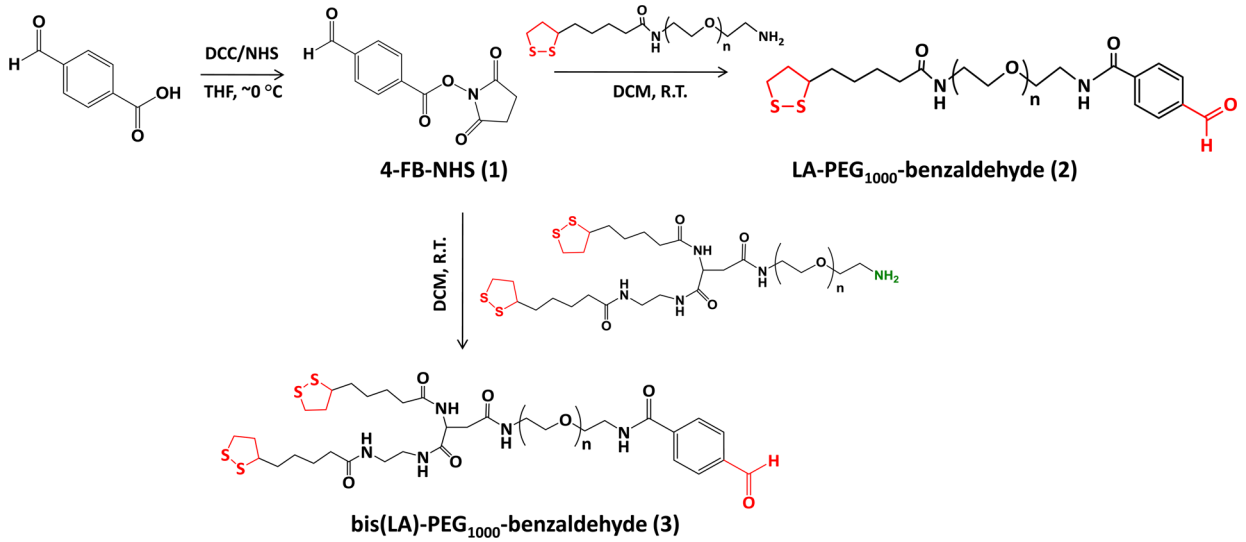

Figure 1. Schematic representation of the chemical structures and synthetic steps to prepare LA-PEG-CHO and bis(LA)-PEG-CHO ligands used in this study.

conditions. They also exhibit minimum interference with the biological properties of the system or cross coupling.[26] Bio-orthogonal reactions applied directly on the nanoparticle surface include strain-promoted azide−alkyne cycloaddition, tetrazine ligation, and hydrazone ligation.[27−30]

For most applications in biology a thorough characterization of the number of target molecules coupled to a nanocrystal (i.e., the surface coverage) following a reaction is crucial. This controls the nanocrystal reactivity and the biological activity of the resulting conjugates. However, characterization of such properties using conventional coupling strategies combined with UV−vis optical spectroscopy, NMR, or ICP-MS spectroscopy has been rather challenging, especially for hydrophilic nanocrystals; results have also been rather limited.[23,31−33] Therefore, it is highly desirable to develop an effective method that can provide quantitative information about the ligand density and reactivity of the nanocrystal surfaces.

In the present study, we report the synthesis of three new PEGylated ligands presenting LA anchors and specific terminal reactive functions: azide-terminated LA-PEG (LA-PEG-N_3), aldehyde-appended LA-PEG (LA-PEG-CHO), and aldehyde-appended bis(LA)-PEG (bis(LA)-PEG-CHO). This design is further combined with a mild photoligation strategy to cap CdSe-ZnS QDs with these ligands under $NaBH_4$-free conditions, providing nanocrystals with controlled surface functionality. The CHO-modified QDs are reacted with 2-hydrazinopyridine (2-HP). This coupling yields hydrazone chromophores with a well-defined optical feature at 350 nm, which has been exploited to extract an estimate for the density of PEG-CHO groups per QD. Similarly, the azide-modified QDs have been reacted with dibenzocyclooctyne (DBCO) via strain-promoted cycloaddition reaction and further coupled with Cy3 dye. The effectiveness of the coupling route is inferred from the combined analyses of the absorption and fluorescence resonance energy transfer data. Furthermore, we have prepared QDs that present both N_3 and CHO groups and used them to test bio-orthogonal coupling (click reaction and hydrazone ligation) on the nanocrystal surfaces.

EXPERIMENTAL SECTION

Materials. Poly(ethylene glycol) (PEG) (MW: ~1000 Da), poly(ethylene glycol) methyl ether (MW: ~750 Da), lipoic acid (LA), 2-hydrozinopyridine (2-HP), 4-formylbenzoic acid (4-FB), *N*-hydroxysuccinimide (NHS), *N*,*N*-dicylohexylcarbodiimide (DCC), tetramethylammonium hydroxide (TMAH), and organic solvents (e.g., $CHCl_3$, CH_2Cl_2, CH_3OH, and C_6H_{14}) were purchased from Sigma Chemicals (St. Louis, MO). Phosphate salts such as monosodium phosphate and disodium phosphate were also purchased from Sigma Chemicals. Poly(ethylene glycol)-modified dibenzocyclooctyne (DBCO-PEG_{200}-NH_2) and sulfo-Cy3 NHS esters were respectively purchased from Click Chemistry Tools (Scottsdale, AZ) and GE Healthcare Life Science (Pittsburgh, PA). Deuterated solvents (e.g., D_2O and $CDCl_3$) used for ^1H NMR and ^{13}C NMR experiments were purchased from Cambridge Isotope Laboratories (Andover, MA). Column chromatography purification was performed using silica gel (60 Å, 230−400 mesh, from Bodman Industries, Aston, PA). All chemical reactions reported here were performed under nitrogen atmosphere unless otherwise specified. Moisture- and oxygen-sensitive solid materials were handled in a glovebox (MBraun Labmaster). All the solvents were used as purchased without further purification, unless otherwise specified.

Instrumentation. The NMR spectra were collected using a Bruker SpectroSpin 600 MHz spectrometer, while the FT-IR (Fourier transform infrared) spectra were recorded on a PerkinElmer FT-IR spectrometer. The optical characterization of the dispersions was carried out using a Shimadzu UV−vis absorption spectrophotometer (UV 2450 model). A Fluorolog-3 spectrometer (JobinYvon Inc., Edison, NJ), equipped with PMT and a CCD for detection, was used to collect the photoluminescence spectra. Solvent evaporation (to concentrate or dry samples) was carried out using a lab-scale Buchi rotary evaporator R-215 (New Castle, DE). The photoligation experiments were carried out using a UV photoreactor, Model LZC-4 V (Luzchem Research Inc., Ottawa, Canada).

LIGAND SYNTHESIS

The various polyethylene glycol-appended monolipoic acid ligands used in this study were prepared following previous protocols with a few modifications.[34] LA-PEG_{750}-OCH_3, bis(LA)-PEG_{750}-OCH_3, and bis(LA)-PEG_{1000}-NH_2 were prepared and purified following the procedures described in our previous reports.[19,35,36] To improve the limited solubility of the azide and aldehyde groups as well as the resulting azide- and aldehyde-functionalized QDs in water, we used a longer

DOI: 10.1021/jacs.5b13574
J. Am. Chem. Soc. 2016, 138, 3190−3201

PEG_{1000} chain (instead of PEG_{400} or PEG_{600}) to prepare both the azide- and aldehyde-appended ligands. As such, the LA-PEG_{1000}-N_3, LA-PEG_{1000}-NH_2, and bis(LA)-PEG_{1000}-NH_2 were synthesized following previous protocols but starting with PEG_{1000} precursor.[34,36] The LA-PEG_{1000}-NH_2 and bis(LA)-PEG_{1000}-NH_2 were further reacted with NHS-activated formylbenzoic acid (4-FB-NHS) to yield LA-PEG_{1000}-CHO and bis(LA)-PEG_{1000}-CHO ligands, as shown in Figure 1. The ligands with various structures and terminal functions were photoligated onto CdSe-ZnS QDs in situ starting with the oxidized form under UV-irradiation.[37] Below we provide the details of the synthetic procedure used for the preparation of the aldehyde-terminated LA-modified ligands.

Compound 1: 4-FB-NHS (NHS-Modified 4-Formylbenzoic Acid). 4-Formylbenzoic acid (1.0 g, ∼ 6.7 mmol), NHS (0.92 g, ∼8 mmol) and 40 mL of THF were mixed in a 250 mL two-neck round-bottom flask equipped with a magnetic stirring bar. The solution was purged with N_2 and cooled to ∼0 °C using an ice bath, and then DCC (1.65 g, ∼8.01 mmol) dissolved in 15 mL of THF was added dropwise. Once the addition was complete, the reaction mixture was gradually warmed up to room temperature and stirred under N_2 atmosphere overnight. The THF was removed using a rotary evaporator, yielding a dry solid, which was redissolved in $CHCl_3$, and the insoluble byproducts (white solid) were removed by passing the solution through a filter paper. The remaining residue was purified using silica gel chromatography employing 20:1 (v/v) $CHCl_3$:MeOH mixture as the eluent. After solvent evaporation, the product was collected as a white solid (∼1.3 g ; reaction yield ∼80%) and stored at 4 °C. ^{1}H NMR (600 MHz, in $CDCl_3$): δ (ppm) 10.13 (s, 1H), 8.29−8.30 (d, 2H, J = 6 Hz), 8.01−8.02 (d, 2H, J = 6 Hz), 2.96 (s, 4H).

Compound 2: LA-PEG-CHO. Compound **1** (4-FB-NHS, 0.21 g, ∼0.85 mmol) was dissolved in 20 mL of DCM in a 100 mL two-neck round-bottom flask. The content was purged with N_2, a solution of LA-PEG_{1000}-NH_2 (1.53 g, 1.27 mmol) dissolved in 20 mL of DCM was added dropwise through an additional funnel at room temperature, and the reaction mixture was stirred overnight. Once the reaction was complete, the mixture was filtered (through a filter paper) to remove any solid byproduct (e.g., NHS). The solution was concentrated using rotary evaporator and further purified on a silica gel column using 20:1 (vol:vol) $CHCl_3$:MeOH solvent mixture as the eluent. The eluted fractions were combined and the solvent was evaporated, yielding compound **2** as a yellow paste (∼1.35 g; reaction yield ∼50%). ^{1}H NMR (600 MHz, in $CDCl_3$): δ (ppm) 10.10 (s, 1H), 7.98−7.99 (d, 2H, J = 6 Hz), 7.91−7.92 (d, 2H, J = 6 Hz), 7.34 (s, 1H), 6.58 (s 1H), 3.62 (m, 90H), 3.52−3.54 (m, 6H), 3.42−3.44 (m, 4H), 3.13−3.17 (m, 1H), 3.06−3.11 (m, 1H), 2.41−2.46 (m, 1H), 2.20 (t, 2H, J = 6 Hz), 1.91−1.85 (m, 1H), 1.63−1.68 (m, 4H), 1.42−1.45 (m, 2H).

Compound 3: Bis(LA)-PEG-CHO. In a 100 mL two-neck round-bottom flask, 4-FB-NHS (0.11 g, ∼0.45 mmol) was dissolved in 15 mL of DCM. Then bis(LA)-PEG_{1000}-NH_2 (1.0 g, ∼0.65 mmol) also dissolved in DCM (15 mL) was added dropwise through an addition funnel. The reaction mixture was stirred at room temperature under N_2 atmosphere overnight. The solution mixture was passed through a filter paper and then further purified on a silica gel column using an eluent mixture of 20:1 (vol:vol) $CHCl_3$:MeOH. The eluted fractions were combined, and the solvent was evaporated, yielding the product as a yellow solid (∼0.5 g; reaction yield ∼50%). ^{1}H NMR (600 MHz, in $CDCl_3$): δ (ppm) 10.10 (s, 1H), 8.03−8.04 (d, 2H), 7.93−7.94 (d, 2H), 7.43 (s, 1H), 6.94 (s 1H), 4.72−4.76 (m, 1H), 3.63 (m, 90 H), 3.52−3.56 (m, 6H), 3.32−3.38 (m, 6H), 3.14−3.20 (m, 2H), 3.07−3.12 (m, 2H), 2.64−2.67 (m, 1H), 2.54−2.57 (m, 1H), 2.40−2.46 (m, 2H), 2.25−2.27 (t, 2H, J = 6 Hz), 2.19−2.21 (t, 2H, J = 6 Hz), 1.85−1.89 (m, 2H), 1.64−1.69 (m, 8H), 1.43−1.48 (m, 4H).

Growth of the Quantum Dots. Growth of the CdSe-ZnS core−shell QDs used in this study was carried out using a stepwise reaction involving the reduction of organometallic precursors at high temperature and in a coordinating solvent mixture made of *n*-trioctylphosphine (TOP), *n*-trioctylphosphine oxide (TOPO), and alkylamines along with a small fraction of *n*-hexylphosphonic acid. Core growth was then followed by overcoating with a few monolayers of ZnS; additional details can be found in previous references.[38−44]

Photoligation of QDs with a Mixture of Azide and Aldehyde-Functionalized Ligands. Below we briefly describe the protocol used to photoligate the CdSe-ZnS QDs with a mixture of LA-PEG_{750}-OCH_3 and LA-PEG_{1000}-CHO (i.e., mixed surface ligand exchange). The molar fraction of LA-PEG_{1000}-CHO used was varied to allow the preparation of QDs with controllable numbers of surface-reactive groups. First, hydrophobic TOP/TOPO-capped QDs (130 μL of a 10 μM stock dispersion in hexane/toluene mixture with a volume ratio of 1:2) were precipitated using excess ethanol, followed by centrifugation, yielding a precipitate of the QD materials; note that the hexane/toluene volume ratio reported above can be slightly varied without affecting the phase transfer process or the quality of the final materials. The solvent was removed using a glass pipet, and the wet QD solid paste was redispersed in 500 μL of hexane. Separately, LA-PEG_{750}-OCH_3 (47.5 mg) and LA-PEG_{1000}-CHO (3.6 mg) were dissolved in 500 μL of MeOH and a catalytic amount of tetramethylammonium hydroxide (TMAH, ∼10 mM) was also added. The content of the two vials (QDs and ligands) were combined in one scintillation vial equipped with a magnetic stirring bar; this yielded a two-phase solution mixture made of a hexane phase containing the QDs (top) and a methanol phase containing the ligands (bottom). The vial was sealed with a rubber septum, and the atmosphere was switched to nitrogen. This vial was placed inside a UV reactor (Luzchem Research Inc., Ottawa, Canada) and then irradiated using UV light (irradiation peak centered at 350 nm and a power = 4.5 mW/cm^2) for 30 min with constant stirring. A complete phase transfer of the QDs from hexane (top) to methanol (bottom) occurred, indicating that ligand exchange had taken place. The organic solvents were removed using a pipet followed by evaporation under vacuum, and then a mixture of chloroform:methanol:hexane (1:1:10, vol:vol:vol) was added to the QD paste followed by centrifugation at 1900*g* for 5 min. The solvent containing TOP, TOPO, and other alkyl amine and alkyl carboxyl ligands were removed using a glass pipet. The QD paste was gently dried under vacuum and dispersed in DI water. Finally, three rounds of concentration/dilution using a centrifugal membrane filtration device (MW cutoff = 50 kDa) were applied to remove excess free hydrophilic and solubilized hydrophobic ligands. This protocol can also be applied to photoligate QDs with other sets of ligands, such as a mixture of LA-PEG_{750}-OCH_3 and LA-PEG_{1000}-N_3, a mixture of bis(LA)-PEG_{750}-OCH_3 and bis(LA)-PEG_{1000}-CHO, or a three-ligand mixture of LA-PEG_{750}-OCH_3, LA-PEG_{1000}-CHO, and LA-PEG_{1000}-N_3. This

DOI: 10.1021/jacs.5b13574
J. Am. Chem. Soc. 2016, 138, 3190−3201

protocol has yielded multifunctional QDs with controllable surface reactivity.

Hydrazone Ligation on Aldehyde-Modified QDs. First, aliquots of QDs photoligated with 5% LA-PEG-CHO (50 μL, 3.67 μM), 2-hydrozinopyridine (2-HP) solution in DMF (7 μL, 1 mg/mL), and 1443 μL of phosphate buffer (10 mM, pH 4.9) were mixed in a scintillation vial. The total volume of the reaction solution was maintained at 1500 μL. Combining the use of excess 2-HP and acidic condition allowed us to increase the reaction yield to ∼100%. The reaction mixture was first placed in a water bath at 37 °C with constant stirring for 2.5 h and then further stirred at room temperature overnight in the dark (by wrapping aluminum foil around the vial). Once the reaction was complete, excess 2-HP was removed by applying one round of centrifugal purification using a membrane filtration device (Amicon, cutoff MW = 50 kDa), and then the solution was concentrated to final volume around 200 μL. The same protocol was applied to attach 2-HP onto QDs photoligated with a higher mole fraction of LA-PEG-CHO, except that the amount of 2-hydrozinopyridine added was accordingly increased. This is done in order to account for the higher density of aldehyde groups per QD and to maintain a 2-HP-to-CHO molar ratio comparable to the one used above. Following the same protocol, different size QDs were photoligated with varying mole fractions of bis(LA)-PEG-CHO (using a mixture of bis(LA)-PEG-CHO and bis(LA)-PEG-OCH_3). Here too, the amount of precursors (e.g., namely 2-hydrozinopyridine) were adjusted to account for the higher fractions of CHO groups per nanocrystal, when larger size nanocrystals with higher surface areas were used.

Click Coupling on Azide-Modified QDs. To implement a strain-promoted metal-free cyclization reaction, 20% LA-PEG-N_3 functionalized QDs (60 μL, 4 μM) and dibenzocyclooctyne-PEG_{200} (DBCO-PEG_{200}-NH_2) stock solution in DMSO (31 μL, 1 mg/mL) were added to a scintillation vial equipped with a magnetic stirring bar. Then 155 μL of phosphate buffer (10 mM, pH 7) and 154 μL of DMSO were added to the vial, and the reaction mixture was stirred at room temperature for 5 h in the dark. Unreacted DBCO was removed using a PD-10 size exclusion column. The first fraction was collected and concentrated to a final volume of ∼150 μL using a centrifugal membrane filtration device (cutoff MW = 50 kDa). The purified sample was mixed with NHS-ester-activated Cy3 predissolved in DMSO (20 μL, 2.4 mM), and then 330 μL of phosphate buffer (10 mM, pH8.7) was added to maintain basic pH condition. The content was stirred at room temperature for 5 h, followed by purification of the final QD-DBCO-dye conjugates using a PD-10 size exclusion column.

Functionalization of QDs with a Mixture of 2-HP and DBCO Groups. A dispersion of QDs photoligated with a mixture of 5% LA-PEG-CHO, 8% LA-PEG-N_3, and 87% LA-PEG-OCH_3 was first prepared. The QDs presenting both azide and aldehyde groups on their surfaces were reacted stepwise with 2-HP and then with DBCO. An aliquot of the QD dispersion (60 μL, 6 μM) was first mixed with 2-HP dissolved in DMF (14 μL, 1 mg/mL), and then 1426 μL of pH4.9 phosphate buffer (10 mM) was added. The reaction was allowed to proceed at 37 °C (using a water bath) for 2.5 h, followed by stirring at room temperature overnight. Once the reaction was complete, excess 2-HP was removed by applying one round of purification using a membrane centrifugal filtration device (cutoff MW = 50 kDa). The purified hydrazinopyridine-modified QDs were reacted with DBCO (1 mg/mL in DMSO, 19 μL) at room temperature and then with NHS-Cy3 dye (1.5 mM in DMSO, 19 μL), following the steps used for the click coupling of azide-QDs described above. The QD-Cy3 conjugates were purified using a PD-10 column. The first fraction was collected and further concentrated using a membrane centrifugal filtration device for further use.

RESULTS AND DISCUSSION

Ligand Design and Phase Transfer. The overall aim of the present ligand design is to introduce aldehyde (CHO) or/and azide (N_3) functional groups on the QD surfaces, with a controllable density and then to use the resulting nanocrystals to implement new coupling chemistries that can selectively and specifically target biomolecules. Such coupling chemistries include hydrazone ligation applied to aldehyde-QDs and strain-promoted cycloaddition carried out using azide-modified QDs. These reactions are reported to be rapid and chemoselective and can proceed without the need for coupling reagents. This contrasts with more "traditional" methods, such as carbodiimide coupling between carboxylic acid and amine groups installed on the targeted molecules. Furthermore, we exploited the high efficiency of the hydrazone ligation and its ability to form a chromophore with a well-defined optical absorption feature, to extract an estimate for the number of LA-PEG and bis(LA)-PEG ligands attached onto a QD. The synthetic protocols of the ligands involve a few simple steps. The LA-PEG_{1000}-N_3 ligands used to prepare azide-functionalized QDs were synthesized following our previous protocols.[14,19,34] Similarly, synthesis of LA-PEG_{1000}-CHO was carried out starting with LA-PEG_{1000}-NH_2. Then, LA-PEG_{1000}-NH_2 was reacted with 4-FB preactivated with NHS (4-FB-NHS-ester), yielding LA-PEG_{1000}-CHO (Figure 1). A similar protocol was applied to prepare bis(LA)-PEG-CHO: bis(LA)-PEG_{1000}-NH_2, prepared using the protocol described in our recent study,[36] was reacted with 4-FB-NHS to provide aldehyde-appended bis(LA)-PEG_{1000} ligands. The use of a longer PEG chain improves the colloidal stability of nanoparticles presenting azide and benzaldehyde groups in aqueous solution;[34] benzaldehyde, in particular, has a limited solubility in water.

Photoligation of QDs with Aldehyde and Azide-Terminated Ligands. The phase transfer of hydrophobic TOP/TOPO-QDs to aqueous media, while preserving the integrity of the target-reactive groups (N_3 and CHO), was achieved using in situ photoligation under sodium borohydride-free conditions and starting with the oxidized form of the ligands. This phase transfer route relies on the photochemical transformation of the lipoic acid groups under UV irradiation at 350 nm. This approach is compatible with an array of LA-based ligands, including small molecules as well as polymer ligands.[19,45,46]

Characterization of the Azide- and Aldehyde-Functionalities on the QDs. We confirmed the intact functionality of the azide and aldehyde groups following photoligation on the QDs using two key analytical tests. (1) The integrity of N_3 groups was verified by comparing the FTIR spectra collected from QDs photoligated with a mixture of 20% LA-PEG-N_3 and 80% LA-PEG-OCH_3 and from pure LA-PEG-N_3 (control). The spectra show that the characteristic band around 2100 cm^{-1} ascribed to N_3 is present in the pure ligand and in the QD samples, indicating that the azide groups have been preserved during the photoligation and phase transfer step (see Supporting Information, Figure S2). The weak intensity of

DOI: 10.1021/jacs.5b13574
J. Am. Chem. Soc. 2016, 138, 3190−3201

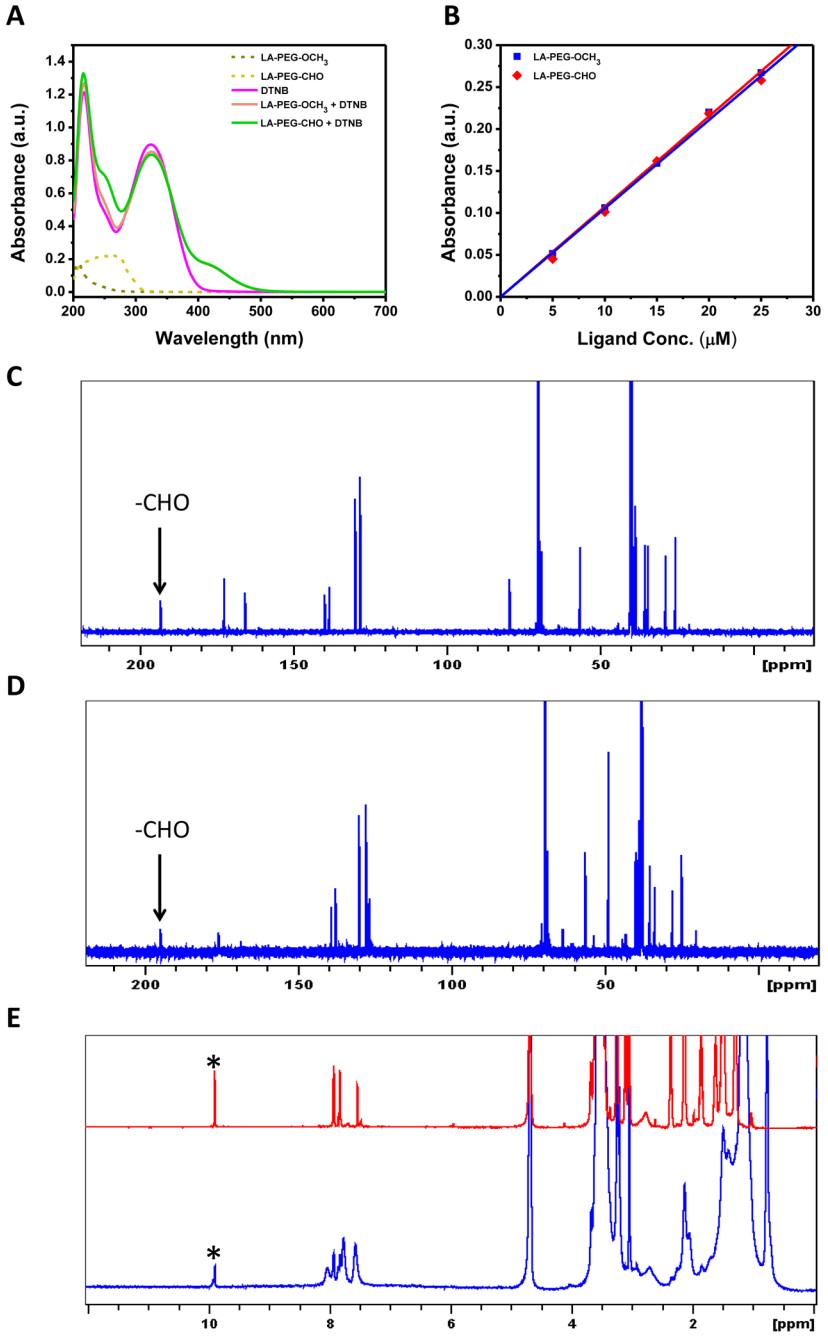

Figure 2. (A) Comparison of the UV−vis absorption spectra collected from solutions of photoirradiated LA-PEG-CHO and LA-PEG-OCH_3 ligands in the presence of 50 μM DTNB; the ligand concentration was 15 μM for both cases. The absorption spectra of DTNB and nonirradiated ligands are also provided. (B) Plot showing the linear correlation between the absorbance at 412 nm (associated with TNB^{2-} product) and the concentration of the photoirradiated ligands; the concentration of the LA-PEG ligands was varied from 5 μM to 25 μM. (C and D) ^{13}C NMR spectra of LA-PEG-CHO ligand in DMSO-d_6 and of photoirradiated LA-PEG-CHO in a deuterated solvent mixture of DMSO-d_6 and D_2O, respectively. (E) ^{1}H NMR spectra of LA-PEG-CHO ligand (red) and QDs photoligated with a mixture of 15% LA-PEG-CHO and 85% LA-PEG-OCH_3 (blue); all the spectra were collected from solutions in D_2O. An asterisk (*) designates the aldehyde feature around 10 ppm.

the N_3 band measured for the QD sample is due to the rather low concentration of QD materials used to collect the FTIR spectrum. (2) We verified the integrity of the aldehyde groups following photoligation on the QDs by checking: (i) the chemical stability of CHO group in the presence of thiol, and (ii) the potential reactivity of CHO with methanol. It is known that aldehyde and ketone can react with thiols to form hemithioacetal and dithioacetal, respectively, which changes the integrity of the carbonyl group. The photoirradiation of LA-based ligands during phase transfer produces abundant active thiol species (e.g., radical byproducts),[47,48] which may react with the aldehyde groups. In addition, methanol solvent (used during photoligation) could react with aldehyde to form hemiacetal or acetal under certain conditions (e.g., neutral conditions). We thus investigated the effect of thiols and methanol on the integrity of the aldehyde using our experimental conditions. The effects of thiol byproducts on the integrity of aldehyde were checked using the Ellman test.

DOI: 10.1021/jacs.5b13574
J. Am. Chem. Soc. 2016, 138, 3190−3201

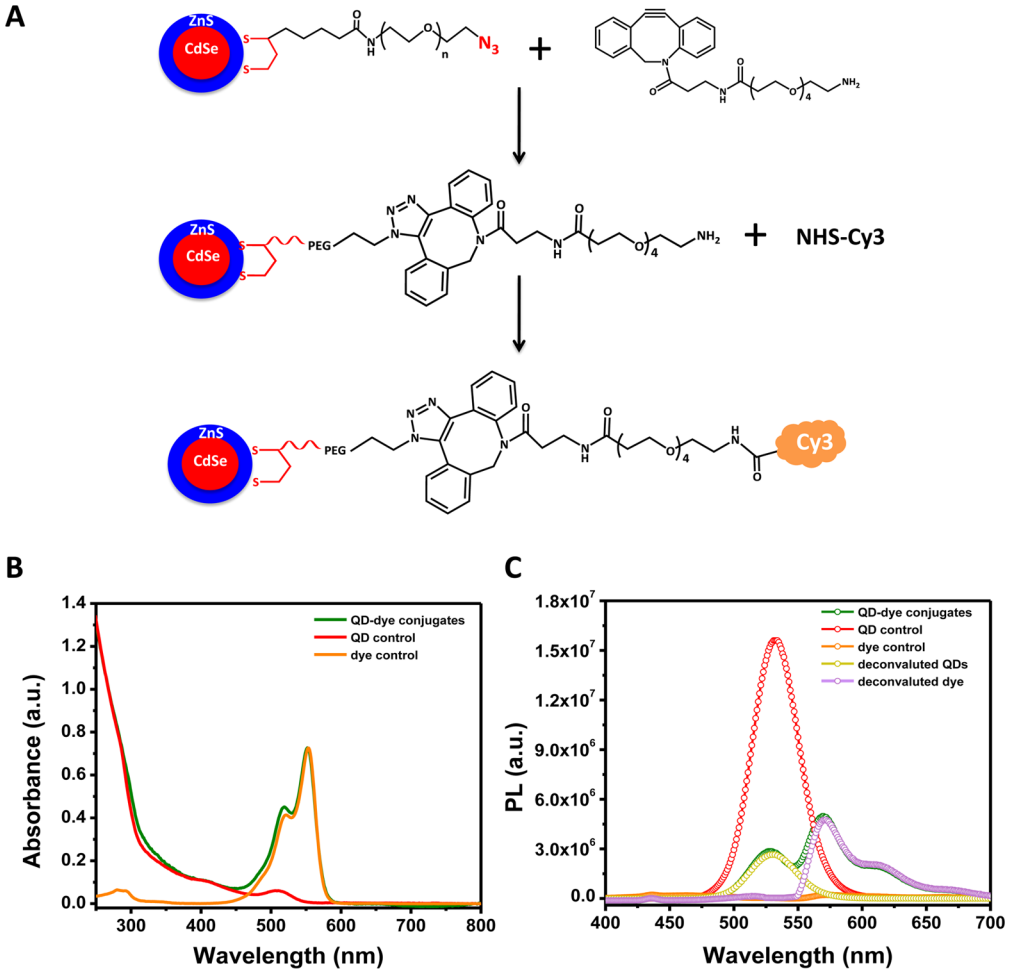

Figure 3. (A) Schematic representation of the QD-Cy3 conjugates assembly via click coupling chemistry. A mixture of LA-PEG-N_3 (20%) and LA-PEG-OCH_3 (80%) was photoligated onto TOP/TOPO-QDs (λ_{em} = 530 nm). The N_3 groups on the QD surfaces were subsequently reacted with DBCO through strain-promoted cycloaddition and then with NHS-Cy3. (B and C) UV−vis absorption and PL spectra of QDs self-assembled with NHS-Cy3. The control samples of QDs and NHS-Cy3 along with the deconvoluted contribution of QDs and NHS-Cy3 are also provided (excitation wavelength = 400 nm).

This test/assay is a reliable route to quantify the concentration of thiol groups in a medium by reacting the thiolated compounds with DTNB (5,5′-dithiobis(2-nitrobenzoic acid)). This reaction yields 5-thio-2-nitrobenzoic acid (TNB^{2-}), a colored product that has a distinct absorption feature at 412 nm (with ε = 14 150 M^{-1} cm^{-1}).[49] Here, the Ellman assay was performed using two sets of ligands: (i) LA-PEG-CHO that was photoirradiated in a MeOH solution purged with argon, and (ii) LA-PEG-OCH_3 irradiated under the same conditions (used as control). We expect that the concentration of free thiols, produced in the irradiated LA-PEG-CHO solution, to be essentially the same as that of LA-PEG-OCH_3 if the generated thiols do not interact with the aldehydes. For this test, a series of solutions with different molar concentrations of LA-PEG-CHO and LA-PEG-OCH_3 (5 μM, 10 μM, 15 μM, 20 μM, 25 μM) in MeOH were prepared and irradiated (at 350 nm using a UV reactor) for 30 min. The samples were then incubated with DTNB (50 μM) for 25 min at room temperature, followed by collection of the absorption spectra. Figure 2A shows one representative example of two different ligand solutions (LA-PEG-CHO and LA-PEG-OCH_3) with the same concentration (15 μM). In both cases, mixing with DTNB produced a new absorbance feature at 412 nm attributed to the product formation, and the absorbance values of the two samples at this wavelength are essentially the same, indicating that photoligation produced the same amount of thiols in the solutions. Moreover, the contribution at 412 nm was found to increase linearly with the ligand concentration. Using this linear correlation between the absorbance at 412 nm and the ligand concentration, we found that the slopes extracted for the two set of ligands are similar, further confirming that the thiols in the medium produced during the photoligation did not interfere with the aldehyde groups (Figure 2B). We should note that the concentration of thiols, determined from the Ellman test data (using Beer's law) for such photochemically transformed ligands, is smaller than the one extracted from chemically reduced DHLA-ligands using sodium borohydride, e.g., the overall concentration of thiol groups produced via photoirradiation of a solution of LA-PEG ligands in methanol is ∼60% of that generated following borohydride-reduction of lipoic acid.[49] Chemical reduction using sodium borohydride has been shown to yield nearly 100% reduction of the dithiolane rings in the sample.[49] In addition, we measured the ^{13}C NMR spectrum of LA-PEG-CHO UV-irradiated in methanol to probe solvent effects; acetal and hemiacetal carbons have clear and distinct signatures in ^{13}C NMR at ∼100 ppm. During the experiment, the LA-PEG-CHO solution in methanol was irradiated for 30 min, and then the methanol was completely

DOI: 10.1021/jacs.5b13574
J. Am. Chem. Soc. 2016, 138, 3190−3201

removed under vacuum (by drying for 3 h). The dried sample was then dissolved in DMSO-d_6 along with a small amount of D_2O; the latter was added to match the aqueous conditions used for reacting the photoligated QDs with 4-FB. The ^{13}C NMR spectra shown in Figure 2C and 2D for nonirradiated and UV-irradiated ligands do not show a signature around 100 ppm (where the expected acetal signature is) but a clearly defined peak at ∼195 ppm, indicating the absence of hemiacetal or acetal from the sample and the presence of the aldehyde. Additionally, the integrity of the aldehyde groups after ligand exchange was characterized by ^1H NMR spectroscopy of CHO-QD dispersion, which shows an aldehyde feature at chemical shift δ = 10.0 ppm (Figure 2E). This is a strong evidence that the integrity of the aldehyde groups on the surface of QDs after photoligation has been preserved, thus paving the way for further coupling with 2-HP.

Strain-Promoted Click Coupling of QDs with DBCO. Conjugation of QDs with biomolecules such as antibodies, enzymes, proteins typically relies on carbodiimide activation chemistry using amine and carboxyl functional groups on the target molecules. One of the disadvantages of this route is that the presence of both amine and carboxyl groups in proteins and antibodies may create undesired cross-linking between the biomolecules, causing aggregation of the desired products (here nanoparticle-conjugates). The recent developments in the use of cycloaddition reaction between azide and alkyne have opened up new opportunities in the modification of nanoparticles for site-specific targeting.[50,51] This reaction meets the criteria of bio-orthogonal chemistry, namely high efficiency and chemoselectivity. Thus far, such conjugation strategy relying on the Cu(I)-catalyzed cycloaddition has been extensively used for the functionalization of Au, silica, and iron oxide nanoparticles.[52−54] When this reaction is applied to QDs, quenching of the emission brought by the copper catalyst (Cu(I)) takes place, rendering its use ineffective, though such quenching can be reduced using a rather thick polymer coating as has been shown recently by Weller and co-workers.[55] The emergence of strain-promoted azide−alkyne cycloaddition (SPAAC) has provided an alternative strategy which relies on the use of highly strained alkynes instead, allowing the reaction to proceed without the need of a copper catalyst. This alternative route has been used to conjugate QDs to target molecules, as described in a few recent reports.[28,56]

In our study, the QDs photoligated with LA-PEG-N_3 were reacted with DBCO-PEG_{200}-NH_2 under mild conditions promoted by SPAAC reaction. To confirm that the reaction between the azide-QDs and alkyne bond in DBCO has taken place, the resulting QD-DBCO conjugates were further coupled to sulfo-Cy3 NHS ester via the reactive amine on the DBCO molecule (see Figure 3A). Figure 3B shows that the absorption spectra of the final conjugates (after purification) display the composite features of both QDs and dye. Additionally, the emission spectra of the conjugates and control samples were measured using 400 nm excitation, which coincides with the absorption valley of Cy3 to minimize direct excitation of acceptor dye. Figure 3C shows that deconvolution of the composite spectrum yields two distinct contributions from the QDs and the dye. Furthermore, the deconvoluted spectra show that the QD contribution has decreased (compared to pure QD dispersion) combined with enhancement in the emission of Cy3; these changes are attributed to efficient FRET interactions. In comparison, the emission signal collected from the Cy3 dye-control was negligible. The combined absorption and emission data provide clear evidence that the QDs and Cy3 were brought in close proximity promoted by covalent coupling, resulting in strong FRET interactions.

We used the above spectroscopic data to extract separate estimates for the number of Cy3 per QD conjugate. First we used the absorption data to estimate the average number of dye (n) attached to a nanocrystal, by comparing the extinction coefficients of the green QDs (3.348×10^5 M^{-1} cm^{-1} at 350 nm) and Cy3 dye (1.5×10^5 M^{-1} cm^{-1} at 552 nm); we extracted a value of $n \sim 9$. We should, however, note that the absorption data alone do not unequivocally prove that conjugation has taken place. FRET measurements, in contrast, are more reliable, because the process requires close proximity interactions.[57] We first extracted the experimental QD-PL quenching efficiency from the emission spectra using the relation:

$$E_n = \frac{F_D - F_{DA}}{F_D} \quad (1)$$

where F_D and F_{DA} represent the emission intensity of the QD-donor alone and QD in the presence of Cy3, respectively. Using a quantum yield (Q_D) value of 0.18, a center-to-center separation distance (r) between QD surface and dye of 60 Å, and a fit to the quenching data assuming a centrosymmetric conjugate configuration, we calculate a valence n of ∼8.[58] This value is in good agreement with the number estimated from the absorption data above. Additional details of the FRET analysis are provided in the Supporting Information.

Hydrazone Ligation and Quantification of the Ligand Density per QD. Exploiting the great potentials offered by inorganic nanoparticles in biology undoubtedly hinges on our ability to understand and control their interactions with biological systems. Such control requires a thorough characterization of the surface properties of such materials, including ligand arrangements, ligand density, and conjugation to target biomolecules.

In an earlier report, we designed maleimide-functionalized AuNPs (by ligand exchanging citrate-nanoparticles with LA-PEG-maleimide ligands).[23] The NPs were reacted with Cy5 dye through a cysteine−peptide bridge and then combined with optical absorption measurements to extract an estimate for the ligand density on two different size AuNPs.[23] One limiting factor of that approach was the difficulty to reduce issues of nonspecific adsorption (i.e., stickiness) of the dye onto the AuNP surfaces. Here, we wanted to exploit the fact that hydrazone ligation between aldehyde groups and hydrazinopyridine can produce a specific chromophore with a well-defined optical signature and use it to extract a measure of the LA-PEG density on luminescent QDs. This strategy can reduce issues of nonspecific adsorption, because the hydrazone chromophores are formed only as a result of a successful ligation reaction. Overall use of this ligand counting strategy benefits from three features: (1) the hydrazone chromophores formed after ligation have a distinct absorption feature at 350 nm, implying that the reaction progress can be monitored optically, (2) the reaction is highly efficient and chemoselective under acidic conditions and without the need for a catalyst,[29,59−61] and (3) the use of hydrazinopyridine derivative to develop new bioconjugation strategies has steadily increased.[62−64] The ligation reaction is carried out in phosphate buffer (pH 4.9). We should stress that use of acidic conditions is crucial for accelerating the ligation reaction, as this pH is reported to enhance the reaction yield

DOI: 10.1021/jacs.5b13574
J. Am. Chem. Soc. 2016, 138, 3190−3201

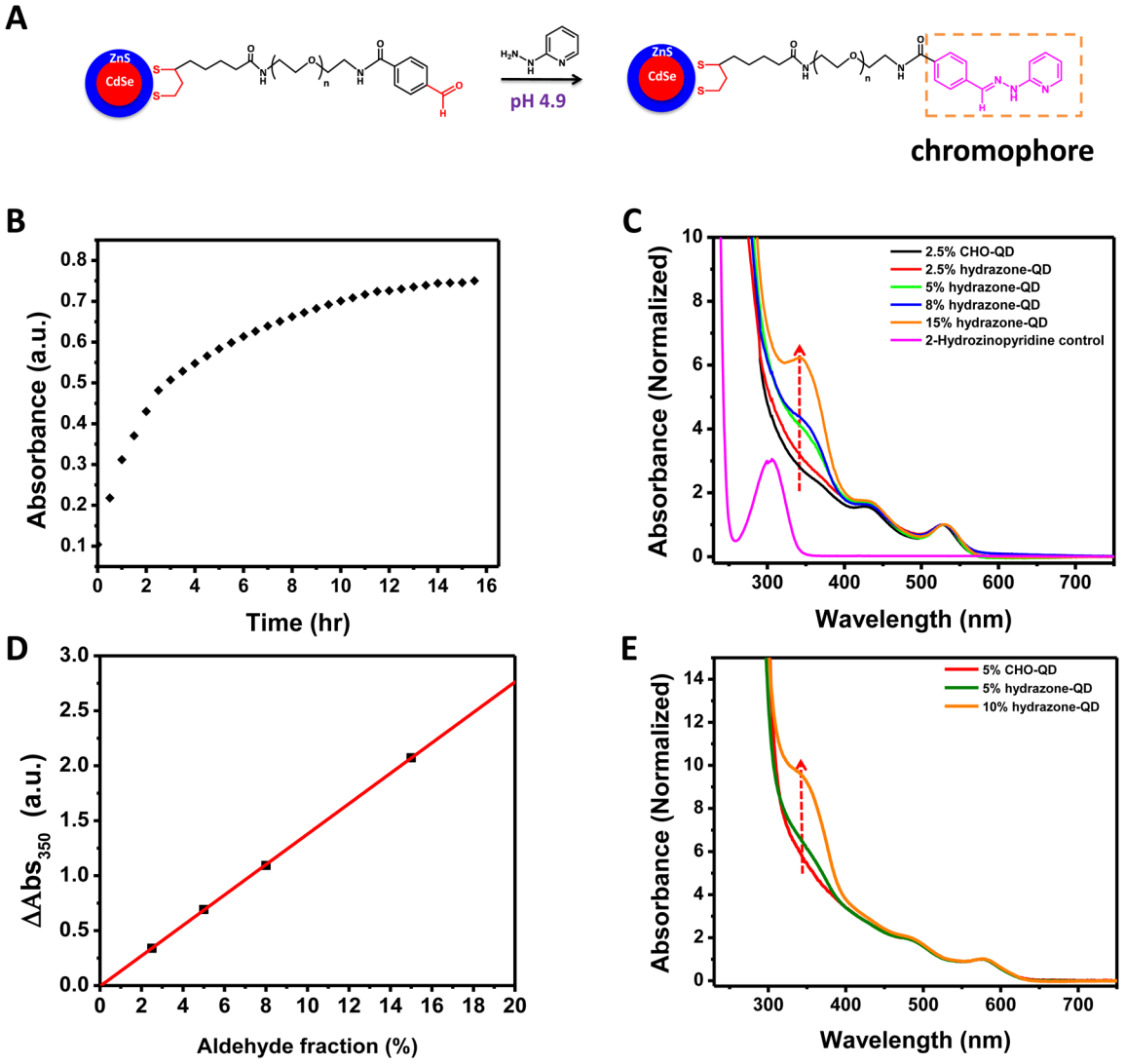

Figure 4. (A) Schematic illustration of the hydrazone ligation applied to prepare QD-hydrazone conjugates. QDs were photoligated with a mixture of LA-PEG-CHO and LA-PEG-OCH_3; the molar fraction of CHO was varied between 2.5 and 15%. The CHO groups on the QD surfaces were covalently ligated with 2-HP, providing hydrazone chromophores with a well-defined feature at 350 nm. (B) Monitoring of the reaction progress with time by tracking the progression of the absorbance at 350 nm: 5% CHO-QDs mixed with 50 times molar excess 2-HP with respect to CHO were used. (C) UV−vis absorption spectra collected from green-emitting (λ_{em} = 540 nm) QD-hydrazone conjugates prepared using CHO-QDs (2.5−15%) reacted with 2-HP; the spectra were collected after removing excess free 2-HP using a membrane filtration device. The absorption spectra of 2-HP alone and 2.5% CHO-QDs were also provided. The absorption spectrum from unreacted CHO-QDs at the corresponding molar fraction is subtracted from every composite spectrum (i.e., of QD-hydazone conjugates) before analysis. (D) Plot of ΔAbs_{350} versus aldehyde molar fraction collected from green-emitting QDs (λ_{em} = 540 nm). (E) UV−vis absorption spectra collected from 5% and 10% bis(LA)-PEG-CHO-QDs ligated with 2-HP, orange-emitting QDs were used (λ_{em} = 590 nm). The absorption spectrum of 5% bis(LA)-PEG-CHO-QDs before ligation is also shown. Absorbance data were collected at room temperature.

over 90% at low reagent concentrations, while eliminating the need for aniline catalyst; the latter quenches the photoluminescence of QDs (see protocol at https://www.hitpages.com/doc/6410955713937408/1/).

To follow the reaction progress, we first investigated its kinetics by tracking changes in the measured absorbance at 350 nm, as coupling between CHO-QDs and 2-HP progressed. Figure 4B shows that the reaction proceeded rapidly during the first 3 h and then gradually slowed down until completion after ~15 h. As a control, we mixed 100% OCH_3-QDs with 2-HP and monitored the absorption at 350 nm under the same reaction conditions. No change in the absorbance at 350 nm was measured regardless of the incubation time, indicating that no hydrazone formation had taken place (see Supporting Information, Figure S3). This can be attributed to the inert nature of the methoxy groups on the QDs. These results prove that hydrazone ligation on the nanocrystal surfaces has taken place only when CHO-QDs were mixed with 2-HP.

We then applied this reaction to two different sets of QDs (with λ_{em} at 540 and 563 nm) photoligated with varying fractions of LA-PEG-CHO. As above, the QD dispersions were reacted with excess amounts of 2-HP to ensure maximal reaction conversion. The reaction mixtures were allowed to proceed for 15 h, and once the reaction was complete, excess 2-HP was removed by applying one round of centrifugal filtration (see Experimental Section). Figure 4C shows that the absorbance at 350 nm increases with increasing fraction of CHO per QD used, due to the formation of hydrazone

DOI: 10.1021/jacs.5b13574
J. Am. Chem. Soc. 2016, 138, 3190−3201

Table 1. Quantification of the Ligand Coverage for Two Different Size QDs Ligated with Mono-LA-PEG[a]

Radius (nm)	λ_{em} (nm)	% aldehyde	# of hydrazone	# of ligands per QD	FPA (nm^2)
3.1	540	2.5	5 ± 2	200 ± 12	~0.60
		5	10 ± 1		
		8	16 ± 1		
		15	30 ± 1		
3.4	563	2.5	7 ± 2	289 ± 38	~0.5
		5	15 ± 1		
		7	20 ± 1		

[a]Shown are the numbers of hydrazone chromophores per QD for each % CHO used, along with the total number of ligands per nanocrystal extracted from fits to the differential absorption data, as detailed in the text. The corresponding FPA values are also shown.

Table 2. Quantification of the Ligand Coverage for a Few Different Size QDs Using Bis(LA)-PEG[a]

radius (nm)	λ_{em} (nm)	% aldehyde	# of hydrazone	# of ligands per QD	FPA (nm^2)
3.1	540	5	6 ± 1	115 ± 16	~1.05
		10	11 ± 1		
3.4	563	5	8 ± 1	155 ± 15	~0.94
		10	15 ± 1		
3.6	590	5	10 ± 1	205 ± 15	~0.79
		10	21 ± 1		
4	630	5	11 ± 1	225 ± 15	~0.89
		10	23 ± 1		

[a]Shown are the numbers of hydrazone chromophores per QD extracted for each CHO fraction used, along with the total number of ligands extracted from the absorption data. The corresponding FPA values are also provided.

chromophores. This contribution is distinct from that of the 2-HP reactant; the latter has a signature at 300 nm (see Figure 4C). Deconvolution of the absorption spectra allowed us to isolate the contribution of the hydrazone chromophores from that of the QDs. The spectrum from a control CHO-QD dispersion prepared with the same molar concentration of QDs (no 2-HP) was subtracted from the composite spectra prior to deconvolution. A plot of the differential absorption at 350 nm (ΔAbs_{350}) vs % CHO used is shown in Figure 4D. The plot shows two important properties of the hydrazone reaction applied to our CHO-functionalized QDs. (1) ΔAbs_{350} exhibits a linear dependence on the %-CHO used, and (2) the linear fit yields a zero intercept at the origin: $\Delta Abs_{350} = \alpha \times$ (% CHO), where α is an experimental constant. The zero intercept is an important feature, as it reflects the high efficiency and specificity of the reaction, combined with the absence of nonspecific binding of the 2-HP groups on the QD surfaces. By comparing the absorbance and the extinction coefficient at 350 nm for the QDs (7.85×10^5 M^{-1} cm^{-1} for 540 nm-emitting QDs and 8.34×10^5 M^{-1} cm^{-1} for 563 nm-emitting QDs) and for the hydrazone chromophore (24 500 M^{-1} cm^{-1}), we extracted an estimate for the number of chromophores formed per QD at each CHO fraction used (see protocol at http://www.solulink.com/products/protocols/4FBColorimetricMSRAssayProteinNanodropMethodProtocol.pdf). In Table 1 we list the number of hydrazone chromophores obtained for different fractions of CHO groups per QD used for green- and yellow-emitting nanocrystals. By extrapolating the linear fit to 100% CHO (corresponding to QDs photoligated with pure LA-PEG-CHO), we extract a measure for the number of ligands per nanocrystal for each size used (see Table 1). Clearly, a larger number of ligands per nanocrystal is measured for the QDs with a larger average surface area: ~200 and 289 ligands per nanocrystal are measured for 540 nm- and 563 nm-emitting QDs, respectively. Additionally, the data show that the footprint area (FPA) per ligand measured for the present QD-ligand pair is ~0.60−0.5 nm^2.

We also applied this ligand counting strategy to QDs capped with bis(LA)-PEG, which has allowed us to investigate the effects of ligand architecture on the capping density. Four different sets of nanocrystals with emission ranging from green to red were photoligated using a mixture of bis(LA)-PEG-OCH_3 (inert) and bis(LA)-PEG-CHO. Following reaction with 2-HP, we extracted values for ΔAbs_{350} vs % CHO per nanocrystal for every set of QDs used. We only used two factions: 5% and 10% CHO-terminated ligands (Figure 4E). Table 2 summarizes the number of hydrazone chromophores measured for each set of QDs as a function of the % CHO used, along with estimates for the total number of bis(LA)-PEG ligands per nanocrystal. The number of ligands per nanocrystal is found to vary with the size for all sets of QDs used. In addition, lower ligand density is measured for bis(LA)-PEG ligands compared with LA-PEG, i.e., the FPA of LA-PEG is ~2 times smaller than that of bis(LA)-PEG. We attribute this difference to the fact that the anchoring motif of the bis(LA)-PEG (with two LA groups) is larger, yielding a lower density coverage compared to mono-LA-PEG.

We should note that introduction of the CHO-appended ligands onto the QD tends to reduce the solubility in buffer media. Indeed, the range of molar fraction of PEG_{1000}-CHO per QD is limited to values smaller than 20%, though such values can vary from one set of QDs to another and from mono-LA-PEG to bis(LA)-PEG ligands. We would also like to note that the major source of errors in estimating the ligand density (and FPA values) result from uncertainty in the measured absorbance values and QD sizes. Uncertainty associated with size estimate may be pronounced for smaller size core−shell nanocrystals. This may affect the FPA values for the green-emitting QDs. The potential effects of crystallinity of the ZnS-

DOI: 10.1021/jacs.5b13574
J. Am. Chem. Soc. 2016, 138, 3190−3201

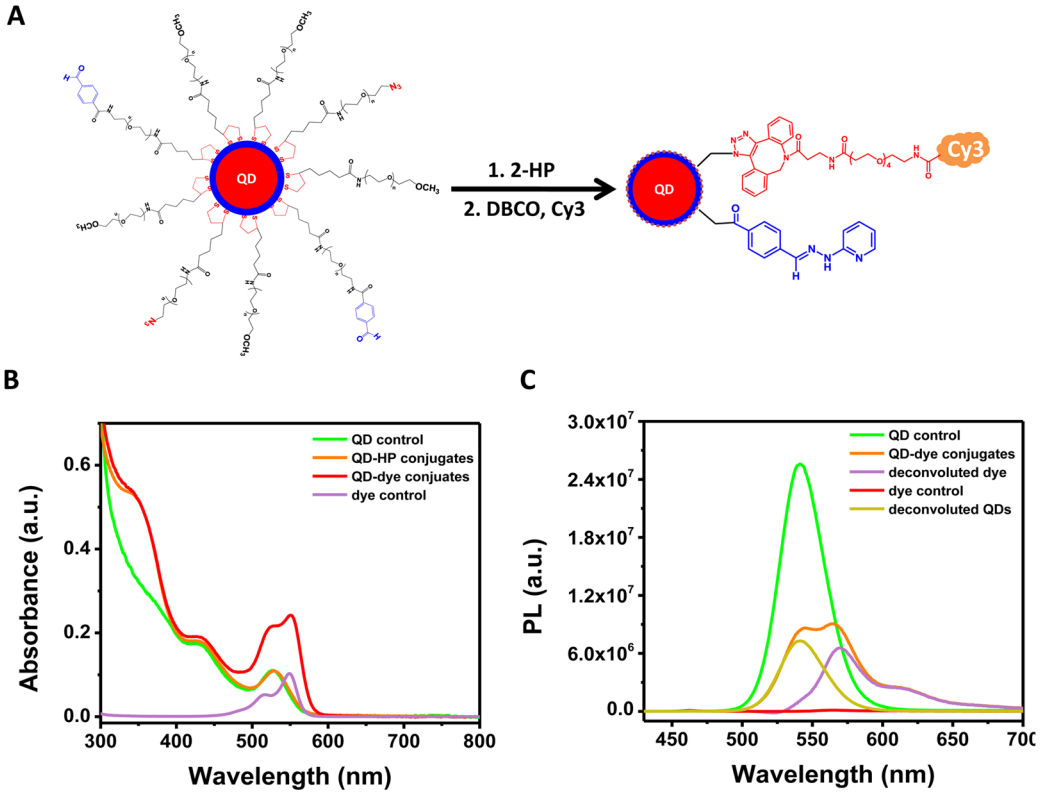

Figure 5. (A) Schematic representation of the stepwise coupling of a QD to 2-HP and DBCO-dye; the starting QD was photoligated with three terminally modified ligands: inert, OCH_3; bio-orthogonal, N_3; CHO. (B) UV–vis absorption spectra of QDs photoligated with 5% LA-PEG-CHO and 8% LA-PEG-N_3, after conjugation with 2-HP and then with NHS-Cy3 dye using DBCO as a bridge; the spectra were collected after purification. (C) PL spectra of QD-Cy3 conjugates, QDs alone, and dye alone, along with the deconvoluted contributions of the QDs and dye (excitation wavelength = 400 nm). Absorbance and fluorescence data were collected at room temperature.

shell, where facets and edges may create somewhat inhomogeneous density of ions at the crystal edge are averaged out. The size difference between the nanocrystals probed is rather small. Finally, we would also like to compare the ligand density measurement using hydrazone ligation to those previously reported by our group using AuNPs, where a dye was conjugated onto a terminal maleimide (on LA-PEG-AuNP) through a peptide bridge. In that study we used the dye absorption to extract an estimate for the FPA value on citrate-AuNPs cap exchanged with LA-PEG ligands. The multistep coupling combined with a rather high degree of nonspecific adsorption had complicated the data analysis, likely yielding lower estimate for the density of LA-PEG ligands on the AuNPs tested.[23]

These findings indicate that combining the use of LA-PEG-aldehyde or bis(LA)-PEG-aldehyde ligands, photoligation strategy, and the hydrazone coupling reaction directly onto the QD surface provides a simple and effective approach to estimate the density of ligands on a nanocrystal. They also indicate that hydrazone ligation is a promising coupling strategy for use in nanoparticle conjugation to various molecules, provided that they are modified with 2-HP derivatives.

Bio-orthogonal Coupling of QDs Modified with Azide and Aldehyde Groups. We started with QDs (λ_{em} = 540 nm) that were photoligated using a mixture of three ligands: 87% LA-PEG-OCH_3, 8% LA-PEG-N_3, and 5% LA-PEG-CHO; this is expected to yield nanocrystals presenting two bio-orthogonal functional/reactive groups (N_3 and CHO). To confirm the presence of the two reactive groups on the QD, the nanocrystals were first reacted with 2-hydrazinopyridine under the reaction conditions mentioned above, purified and the absorption spectrum was collected. Figure 5B shows that there is clear enhancement in the absorbance at 350 nm compared to the QD control, confirming that hydrazone chromophores have been formed. This provides strong evidence that the aldehyde groups were present on the QD surfaces and were readily accessible for reaction with the hydrazine derivative. The resulting QD-2-hydrazinopyridine conjugates were then reacted with DBCO-PEG_{200}-NH_2 followed by reaction with NHS-Cy3 dye. The absorption spectrum collected from the final dispersion (after purification using a PD-10 column) shows a clear contribution from both QDs and Cy3 dye (Figure 5B). Similarly, the composite emission spectrum also shows contributions from the QDs at 540 nm and Cy3 at 570 nm (see Figure 5C). Furthermore, there is substantial reduction of the QD signal compared to that measured for the QDs-only sample. A control experiment of Cy3 alone with the same concentration provides a negligible PL signal compared to the contribution measured for the conjugates. These features indicate that resonance energy transfer has taken place as a result of covalent binding between the QD-azide-DBCO and NHS-Cy3.

These above results indicate that our ligand design combined with the photoligation and mixed surface coating strategy have the potential for developing multifunctional nanoparticles that combine multiple bio-orthogonal functionalities on a single nanoscale platform. The process is simple to implement, and the introduction of the two reactive groups onto the QD surfaces can be achieved during ligand exchange and without the need for post phase transfer modification. The resulting

DOI: 10.1021/jacs.5b13574
J. Am. Chem. Soc. 2016, 138, 3190–3201

bio-orthogonal platforms constitute an improvement over monofunctional nanoparticles and can be applied to target two different biomolecules with the desired functions via highly efficient coupling chemistries.

CONCLUSION

We have designed and synthesized modular multidentate ligands with terminal azide or aldehyde reactivity. The ligand design uses lipoic acid as anchors and was combined with a mild photoligation strategy to prepare azide- and aldehyde-functionalized QDs with controllable reactivity. The azide-modified QDs were reacted with dibenzocyclooctyne via click reaction under Cu(I)-free conditions, eliminating issues of QD PL losses encountered when the coupling requires the use of copper catalyst. We also covalently coupled aldehyde-functionalized QDs with 2-hydrozinopyridine, leading to the formation of hydrazone chromophores, with a well-defined optical signature, on the QD surface. This route has eliminated problems associated with nonspecific stickiness routinely encountered when attaching dyes or other analytical labels via conventional coupling chemistries.

We exploited the specific optical feature of the hydrazone chromophore at 350 nm to estimate the number of chromophores formed on a QD when the mole fraction of aldehydes was changed. We found that the number of chromophores per QD linearly tracked the % CHO introduced on the nanocrystal. This allowed us to extract a measure for the number of ligands per QD for a few sets of nanocrystals emitting at distinct regions of the optical spectrum. We further used this strategy to explore the effects of ligand architecture on the density of surface coverage by comparing mono-LA-appended vs bis(LA)-appended PEG ligands and found that the ligand density coverage was indeed strongly dependent on the ligand architecture but not on the nanocrystal size. Using mixed ligation, we prepared multifunctional QDs that combine azide and aldehyde functionalities on the same nanocrystal and showed that the resulting nanocrystals can be easily reacted with two specific target molecules with no cross-reactivity. This strategy can be easily applied to other nanoparticles. The ability to provide nanoparticles presenting aldehyde and azide groups on the same platforms is greatly promising for a variety of applications in biology. They provide multifunctional platforms which can be used as probes and/or carriers in applications such as imaging, diagnostics, sensing, and delivery.

ASSOCIATED CONTENT

Supporting Information

The Supporting Information is available free of charge on the ACS Publications website at DOI: 10.1021/jacs.5b13574.

Additional details on the Förster dipole−dipole analysis applied to the energy transfer data, NMR and FT-IR spectra of aldehyde- and azide-modified ligands and QDs, and tracking of the reaction progression with time (PDF)

AUTHOR INFORMATION

Corresponding Author

*mattoussi@chem.fsu.edu

Notes

The authors declare no competing financial interest.

ACKNOWLEDGMENTS

We thank the National Science Foundation for financial support (NSF-CHE no. 1508501 and no. 1058957). We also thank Professor Philip E. Dawson and Dr. Valle Palomo (at the Scripps Research Institute) for fruitful discussions.

REFERENCES

(1) Larson, D. R.; Zipfel, W. R.; Williams, R. M.; Clark, S. W.; Bruchez, M. P.; Wise, F. W.; Webb, W. W. *Science* **2003**, *300*, 1434.
(2) Medintz, I.; Uyeda, H.; Goldman, E.; Mattoussi, H. *Nat. Mater.* **2005**, *4*, 435.
(3) Michalet, X.; Pinaud, F.; Bentolila, L.; Tsay, J.; Doose, S.; Li, J.; Sundaresan, G.; Wu, A.; Gambhir, S.; Weiss, S. *Science* **2005**, *307*, 538.
(4) Zrazhevskiy, P.; Sena, M.; Gao, X. H. *Chem. Soc. Rev.* **2010**, *39*, 4326.
(5) Nam, J.; Won, N.; Bang, J.; Jin, H.; Park, J.; Jung, S.; Jung, S.; Park, Y.; Kim, S. *Adv. Drug Delivery Rev.* **2013**, *65*, 622.
(6) Cassette, E.; Helle, M.; Bezdetnaya, L.; Marchal, F.; Dubertret, B.; Pons, T. *Adv. Drug Delivery Rev.* **2013**, *65*, 719.
(7) Mattoussi, H.; Palui, G.; Na, H. B. *Adv. Drug Delivery Rev.* **2012**, *64*, 138.
(8) Wu, X. Y.; Liu, H. J.; Liu, J. Q.; Haley, K. N.; Treadway, J. A.; Larson, J. P.; Ge, N. F.; Peale, F.; Bruchez, M. P. *Nat. Biotechnol.* **2003**, *21*, 41.
(9) Pellegrino, T.; Manna, L.; Kudera, S.; Liedl, T.; Koktysh, D.; Rogach, A. L.; Keller, S.; Radler, J.; Natile, G.; Parak, W. J. *Nano Lett.* **2004**, *4*, 703.
(10) Uyeda, H. T.; Medintz, I. L.; Jaiswal, J. K.; Simon, S. M.; Mattoussi, H. *J. Am. Chem. Soc.* **2005**, *127*, 3870.
(11) Lees, E. E.; Nguyen, T. L.; Clayton, A. H. A.; Mulvaney, P.; Muir, B. W. *ACS Nano* **2009**, *3*, 1121.
(12) Liu, W. H.; Greytak, A. B.; Lee, J.; Wong, C. R.; Park, J.; Marshall, L. F.; Jiang, W.; Curtin, P. N.; Ting, A. Y.; Nocera, D. G.; Fukumura, D.; Jain, R. K.; Bawendi, M. G. *J. Am. Chem. Soc.* **2010**, *132*, 472.
(13) Mattoussi, H.; Mauro, J. M.; Goldman, E. R.; Anderson, G. P.; Sundar, V. C.; Mikulec, F. V.; Bawendi, M. G. *J. Am. Chem. Soc.* **2000**, *122*, 12142.
(14) Susumu, K.; Uyeda, H. T.; Medintz, I. L.; Pons, T.; Delehanty, J. B.; Mattoussi, H. *J. Am. Chem. Soc.* **2007**, *129*, 13987.
(15) Liu, W.; Howarth, M.; Greytak, A. B.; Zheng, Y.; Nocera, D. G.; Ting, A. Y.; Bawendi, M. G. *J. Am. Chem. Soc.* **2008**, *130*, 1274.
(16) Liu, W. H.; Choi, H. S.; Zimmer, J. P.; Tanaka, E.; Frangioni, J. V.; Bawendi, M. *J. Am. Chem. Soc.* **2007**, *129*, 14530.
(17) Muro, E.; Pons, T.; Lequeux, N.; Fragola, A.; Sanson, N.; Lenkei, Z.; Dubertret, B. *J. Am. Chem. Soc.* **2010**, *132*, 4556.
(18) Stewart, M. H.; Susumu, K.; Mei, B. C.; Medintz, I. L.; Delehanty, J. B.; Blanco-Canosa, J. B.; Dawson, P. E.; Mattoussi, H. *J. Am. Chem. Soc.* **2010**, *132*, 9804.
(19) Zhan, N.; Palui, G.; Mattoussi, H. *Nat. Protoc.* **2015**, *10*, 859.
(20) Delgado, C.; Francis, G. E.; Fisher, D. *Crit. Rev. Ther. Drug Carrier Syst.* **1992**, *9*, 249.
(21) Palui, G.; Na, H. B.; Mattoussi, H. *Langmuir* **2012**, *28*, 2761.
(22) Dixit, V.; Van den Bossche, J.; Sherman, D. M.; Thompson, D. H.; Andres, R. P. *Bioconjugate Chem.* **2006**, *17*, 603.
(23) Oh, E.; Susumu, K.; Blanco-Canosa, J. B.; Medintz, I. L.; Dawson, P. E.; Mattoussi, H. *Small* **2010**, *6*, 1273.
(24) Zhang, C. Y.; Yeh, H. C.; Kuroki, M. T.; Wang, T. H. *Nat. Mater.* **2005**, *4*, 826.
(25) Hermanson, G. T. *Bioconjugate Techniques*, 3rd ed.; Academic Press: New York, 2013, 1.
(26) Prescher, J. A.; Bertozzi, C. R. *Nat. Chem. Biol.* **2005**, *1*, 13.
(27) Bernardin, A.; Cazet, A.; Guyon, L.; Delannoy, P.; Vinet, F.; Bonnaffe, D.; Texier, I. *Bioconjugate Chem.* **2010**, *21*, 583.
(28) Zhang, P.; Liu, S.; Gao, D.; Hu, D.; Gong, P.; Sheng, Z.; Deng, J.; Ma, Y.; Cai, L. *J. Am. Chem. Soc.* **2012**, *134*, 8388.
(29) Blanco-Canosa, J. B.; Medintz, I. L.; Farrell, D.; Mattoussi, H.; Dawson, P. E. *J. Am. Chem. Soc.* **2010**, *132*, 10027.

DOI: 10.1021/jacs.5b13574
J. Am. Chem. Soc. 2016, 138, 3190−3201

(30) Han, H. S.; Devaraj, N. K.; Lee, J.; Hilderbrand, S. A.; Weissleder, R.; Bawendi, M. G. *J. Am. Chem. Soc.* **2010**, *132*, 7838.
(31) Liu, X.; Yu, M.; Kim, H.; Mameli, M.; Stellacci, F. *Nat. Commun.* **2012**, *3*, article number 1182.
(32) Mullen, D. G.; Fang, M.; Desai, A.; Baker, J. R.; Orr, B. G.; Holl, M. M. B. *ACS Nano* **2010**, *4*, 657.
(33) Hinterwirth, H.; Kappel, S.; Waitz, T.; Prohaska, T.; Lindner, W.; Lammerhofer, M. *ACS Nano* **2013**, *7*, 1129.
(34) Susumu, K.; Mei, B. C.; Mattoussi, H. *Nat. Protoc.* **2009**, *4*, 424.
(35) Mei, B. C.; Susumu, K.; Medintz, I. L.; Mattoussi, H. *Nat. Protoc.* **2009**, *4*, 412.
(36) Zhan, N.; Palui, G.; Kapur, A.; Palomo, V.; Dawson, P. E.; Mattoussi, H. *J. Am. Chem. Soc.* **2015**, *137*, 16084.
(37) Zhan, N. Q.; Palui, G.; Safi, M.; Ji, X.; Mattoussi, H. *J. Am. Chem. Soc.* **2013**, *135*, 13786.
(38) Dabbousi, B. O.; RodriguezViejo, J.; Mikulec, F. V.; Heine, J. R.; Mattoussi, H.; Ober, R.; Jensen, K. F.; Bawendi, M. G. *J. Phys. Chem. B* **1997**, *101*, 9463.
(39) Peng, Z. A.; Peng, X. G. *J. Am. Chem. Soc.* **2001**, *123*, 183.
(40) Murray, C. B.; Norris, D. J.; Bawendi, M. G. *J. Am. Chem. Soc.* **1993**, *115*, 8706.
(41) Murray, C. B.; Kagan, C. R.; Bawendi, M. G. *Annu. Rev. Mater. Sci.* **2000**, *30*, 545.
(42) Hines, M. A.; Guyot-Sionnest, P. *J. Phys. Chem.* **1996**, *100*, 468.
(43) Qu, L. H.; Peng, Z. A.; Peng, X. G. *Nano Lett.* **2001**, *1*, 333.
(44) Clapp, A. R.; Goldman, E. R.; Mattoussi, H. *Nat. Protoc.* **2006**, *1*, 1258.
(45) Wang, W.; Kapur, A.; Ji, X.; Safi, M.; Palui, G.; Palomo, V.; Dawson, P. E.; Mattoussi, H. *J. Am. Chem. Soc.* **2015**, *137*, 5438.
(46) Palui, G.; Avellini, T.; Zhan, N.; Pan, F.; Gray, D.; Alabugin, I.; Mattoussi, H. *J. Am. Chem. Soc.* **2012**, *134*, 16370.
(47) Bucher, G.; Lu, C. Y.; Sander, W. *ChemPhysChem* **2005**, *6*, 2607.
(48) Brown, P. R.; Edwards, J. O. *J. Org. Chem.* **1969**, *34*, 3131.
(49) Aldeek, F.; Hawkins, D.; Palomo, V.; Safi, M.; Palui, G.; Dawson, P. E.; Alabugin, I.; Mattoussi, H. *J. Am. Chem. Soc.* **2015**, *137*, 2704.
(50) Lutz, J.-F.; Zarafshani, Z. *Adv. Drug Delivery Rev.* **2008**, *60*, 958.
(51) Lim, R. K. V.; Lin, Q. *Chem. Commun.* **2010**, *46*, 1589.
(52) Nebhani, L.; Barner-Kowollik, C. *Adv. Mater.* **2009**, *21*, 3442.
(53) Na, H. B; Palui, G.; Rosenberg, J. T.; Ji, X.; Grant, S. C.; Mattoussi, H. *ACS Nano* **2012**, *6*, 389.
(54) Brennan, J. L.; Hatzakis, N. S.; Tshikhudo, T. R.; Dirvianskyte, N.; Razumas, V.; Patkar, S.; Vind, J.; Svendsen, A.; Nolte, R. J. M.; Rowan, A. E.; Brust, M. *Bioconjugate Chem.* **2006**, *17*, 1373.
(55) Ostermann, J.; Merkl, J. P.; Flessau, S.; Wolter, C.; Kornowksi, A.; Schmidtke, C.; Pietsch, A.; Kloust, H.; Feld, A.; Weller, H. *ACS Nano* **2013**, *7*, 9156.
(56) Schieber, C.; Bestetti, A.; Lim, J. P.; Ryan, A. D.; Nguyen, T.-L.; Eldridge, R.; White, A. R.; Gleeson, P. A.; Donnelly, P. S.; Williams, S. J.; Mulvaney, P. *Angew. Chem., Int. Ed.* **2012**, *51*, 10523.
(57) Lakowicz, J. R. *Principles of Fluorescence Spectroscopy*, 3rd ed.; Springer: New York, 2006.
(58) Ji, X.; Wang, W.; Mattoussi, H. *Phys. Chem. Chem. Phys.* **2015**, *17*, 10108.
(59) Jencks, W. P. *J. Am. Chem. Soc.* **1959**, *81*, 475.
(60) Nilsson, B. L.; Hondal, R. J.; Soellner, M. B.; Raines, R. T. *J. Am. Chem. Soc.* **2003**, *125*, 5268.
(61) Dirksen, A.; Dirksen, S.; Hackeng, T. M.; Dawson, P. E. *J. Am. Chem. Soc.* **2006**, *128*, 15602.
(62) Aryal, S.; Grailer, J. J.; Pilla, S.; Steeber, D. A.; Gong, S. *J. Mater. Chem.* **2009**, *19*, 7879.
(63) Iyer, G.; Pinaud, F.; Xu, J.; Ebenstein, Y.; Li, J.; Chang, J.; Dahan, M.; Weiss, S. *Bioconjugate Chem.* **2011**, *22*, 1006.
(64) Hong, Z.-Y.; Lv, C.; Liu, A.-A.; Liu, S.-L.; Sun, E.-Z.; Zhang, Z.-L.; Lei, A.-W.; Pang, D.-W. *ACS Nano* **2015**, *9*, 11750.

DOI: 10.1021/jacs.5b13574
J. Am. Chem. Soc. 2016, 138, 3190−3201